

# Construction of 1D $\pi$ -Stacked Superstructures with Inclusion Channels through Symmetry-Decreasing Crystallization of Discotic Molecules of $C_3$ Symmetry

Ichiro Hisaki,<sup>\*[a]</sup> Hirofumi Senga,<sup>[a]</sup> Hajime Shigemitsu,<sup>[a]</sup> Norimitsu Tohnai,<sup>[a, b]</sup> and Mikiji Miyata<sup>\*[a]</sup>

A 1D  $\pi$ -stacked columnar assembly composed of discotic  $\pi$ -conjugated molecules is one of the key architectures of organic semiconductor materials. To date, attractive properties, such as energy transfer and charge-carrier mobility, have been reported for the architectures of polycyclic aromatic hydrocarbons, porphyrin, phthiocianine, and acetylene-bridged macrocycles.<sup>[1]</sup> In connection to this, we became interested in construction of supramolecular architectures with both 1D  $\pi$ -stacked columns and inclusion channels (abbreviated as 1D- $\pi$ S-IC superstructure), because optical and electrical properties of these 1D assemblies are expected to be tuned by additional molecules accommodated in the channels, and moreover, absorption and desorption of the molecules may lead to dynamic changes of the properties. The 1D- $\pi$ S-IC superstructures have recently been achieved in covalent organic frameworks (COF).<sup>[2–4]</sup> On the other hand, noncovalently linked 1D- $\pi$ S-IC systems formed through weak interactions are still rare,<sup>[5]</sup> although such systems are expected to show more dynamic structural change and physical-property modulation compared with covalently linked systems.

To generate inclusion spaces in a molecular assembly, molecules with  $C_3$  symmetry are often applied,<sup>[6–9]</sup> because it is easy to image that they can give assemblies with hexagonal or trigonal void space (Figure 1a and b, respectively) when they experience symmetry carry-over crystallization.<sup>[10]</sup> Formation of these superstructures, however, are frequently thwarted by offset-mannered stacking of the molecule that does not give infinite channels, but discrete void spaces.<sup>[8]</sup>

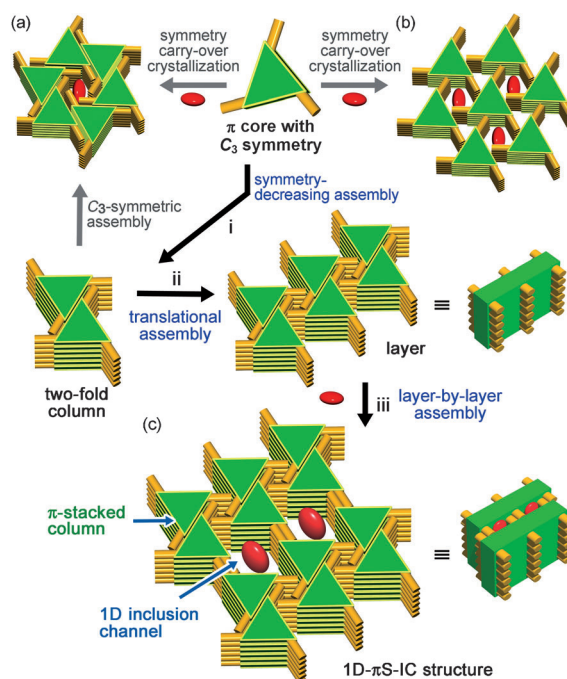


Figure 1. Schematic representation for construction of 1D,  $\pi$ -stacked, columnar architectures with inclusion channels composed of a discotic molecule with  $C_3$  symmetry: a) Hexagonal and b) trigonal arrangements formed through symmetry carry-over crystallization. c) A layer-by-layer arrangement with rhombic inclusion channels formed through a symmetry-decreasing crystallization. The hierarchical scenario for a layer-by-layer superstructure formation involves the following processes: i) formation of two-fold column, ii) layer formation by translational assembly of the column, and iii) lamination of the layer accompanied by guest inclusion into the space surrounded by the other arm.

[a] Dr. I. Hisaki, H. Senga, H. Shigemitsu, Dr. N. Tohnai,

Prof. Dr. M. Miyata

Department of Material and Life Science

Graduate School of Engineering, Osaka University

2-1 Yamadaoka, Suita, Osaka 565-0871 (Japan)

Fax: (+81) 6-6879-7406

E-mail: hisaki@mls.eng.osaka-u.ac.jp

miyata@mls.eng.osaka-u.ac.jp

[b] Dr. N. Tohnai

Japan Science and Technology Agency (JST)

PRESTO, 4-1-8 Honcho, Kawaguchi, Saitama 332-0011 (Japan)

Supporting information for this article is available on the WWW under <http://dx.doi.org/10.1002/chem.201103133>.

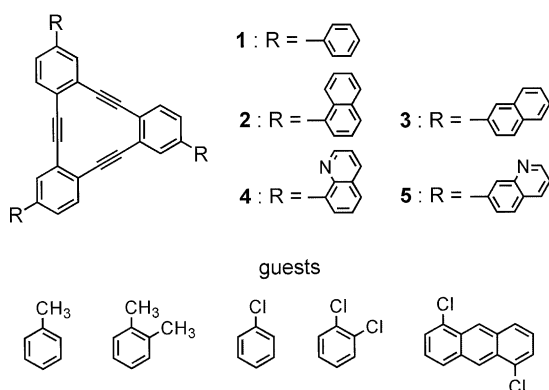
Therefore, herein, we planned to construct the 1D- $\pi$ S-IC superstructure by symmetry-decreasing crystallization of a  $C_3$  molecule with rigid aromatic arms in the periphery (Figure 1c). The term we propose—symmetry-decreasing crystallization—denotes crystallization when high-symmetry molecules adopt crystal structures with lower symmetry. A scenario of the crystallization in this study is hierarchically described as follows: i) Two  $C_3$  molecules form a two-fold symmetric dimer so as to maximize their van der Waals contacts provided by the core and two arms.<sup>[11]</sup> Subsequently,

the dimers stack to form a two-fold columnar assembly. ii) The two-fold columns align to form a layer, which has projecting arms as pillars on its surface. iii) The layers stack; this is accompanied by guest inclusion into void spaces surrounded by the pillars to form the 1D- $\pi$ S-IC superstructure.

Discotic hexadehydrotribenzo[12]annulene (DBA)<sup>[12]</sup> with  $C_3$  symmetry seems to be an appropriate compound for the  $\pi$ -conjugated core, because a  $\pi$ -stacked 1D superstructure of a DBA derivative was revealed to exhibit significant anisotropic hole-carrier mobility along the columnar axis.<sup>[13]</sup> Furthermore, DBA derivatives have been applied as building blocks of various supramolecular architectures, including vesicles,<sup>[14]</sup> columnar liquid crystals,<sup>[15]</sup> and porous 2D networks on a highly oriented pyrolytic graphite (HOPG) surface.<sup>[16]</sup>

Herein, we first demonstrate that the 1D- $\pi$ S-IC superstructures of DBA derivatives with  $C_3$  symmetry are established by symmetry-decreasing crystallization. Particularly, 2-naphthyl-armed DBA gave a framework that exhibited a relatively wide channel with walls of the naphthyl plane. The channel is capable of accommodating various aromatic guests through CH- $\pi$  or Cl- $\pi$  contacts with the walls. Furthermore, some crystals dynamically release the included guest molecules even under ambient conditions, with accompanying structural changes.

DBAs **1–5** were synthesized according to Scheme 1. Recrystallization of the DBAs was performed in the presence of various aromatic compounds to give inclusion crystals.<sup>[17]</sup>



Scheme 1. DBA derivatives with rigid aromatic arms and aromatic guests included in 1D channels.

Contrary to the DBA crystals with the space groups of  $R\bar{3}c$  and  $R\bar{3}c$ , which we have reported previously,<sup>[8c]</sup> the present systems gave crystal structures with lower symmetry. Namely, DBA **1**<sup>[8c]</sup> yielded a  $P\bar{1}$  crystal that did not include any aromatic molecules, but that did include chloroform (**1·CHCl<sub>3</sub>**) with a 2:1 host/guest molar ratio. DBA **2**, on the other hand, gave a  $P\bar{1}$  crystal that included toluene (**2·Tol**) with a 1:1 host/guest molar ratio. DBA **3** gave  $P2_1/c$  crystals that included toluene, *o*-xylene, chlorobenzene, and *o*-dichlorobenzene, (**3·Tol**, **3·Xyl**, **3·ClBen**, and **3·Cl<sub>2</sub>Ben**, respec-

tively) with a 1:1 host/guest molar ratio, and 1,5-dichloroanthracene (**3·Cl<sub>2</sub>Ant**) with a 2:1 host/guest ratio. In these structures, spontaneous formation of both 1D stacked DBA superstructures and 1D inclusion spaces were successfully achieved. Quinoline-armed DBAs **4** and **5**, to our dismay, did not yield any inclusion crystals despite of many trials; **4** formed a guest-free crystal (Figure S1, Table S1 in the Supporting Information) and **5** has not yet given any crystals, but amorphous materials.

In Figure 2, crystal structures of **1·CHCl<sub>3</sub>**, **2·Tol**, and **3·Tol** are shown. The **1·CHCl<sub>3</sub>** crystal exhibits a pseudo-two-fold 1D columnar structure of DBA along the *a* axis. The dimeric column aligns along the diagonal direction of the *bc* plane to give a layer, which stacks along the *b* axis, and a crystal with 1D- $\pi$ S-IC superstructure (Figure 2a). The fact that only chloroform molecules are accommodated in the narrow inclusion spaces surrounded by rotationally disordered phenyl groups indicates that a phenyl group is too small as a pillar to generate inclusion space. Naphthalene-armed DBAs **2** and **3**, on the other hand, achieved obvious 1D- $\pi$ S-IC superstructures without disorder of the host frameworks. The arms of DBA **2** are largely twisted from the DBA plane by 51.8–72.6° (Figure S2 in the Supporting Information) because of steric repulsion between the hydrogen atoms at *peri*-positions of the naphthyl group and those of the DBA ring. Therefore, the rhombic dimeric pair is not formed. DBA **2** is slipped stacked with a small  $\pi$  overlap to form a column. The columns align to form two types of narrow inclusion channels (A) and (B) with dimensions of approximately 3.7×4.3 and 6.8×3.1 Å<sup>2</sup>, respectively (Figure 2b). Contrary to the 1-naphthyl moieties in **2**, the 2-naphthyl groups in **3** are less hindered, and therefore, twisted from the DBA plane with smaller angles of 1.7–32.6°. Naphthyl arms **I** and **II** take part in the widely spread edge-to-face CH- $\pi$  contact with the adjacent molecule (Figure 2c) to form a two-fold helical column. The column aligns along the *c* axis to form a layer, and the layer stacks along the *a* axis to form an inclusion channel, with dimensions of approximately 5.2×9.0 Å<sup>2</sup>, surrounded by the other naphthyl arm (**III**). In the channels, toluene molecules are slipped stacked in two rows.

Furthermore, we succeeded in revealing crystal structures of **3·Xyl**, **3·ClBen**, **3·Cl<sub>2</sub>Ben**, and **3·Cl<sub>2</sub>Ant**, which have quite similar porous frameworks with that of **3·Tol**. However, recrystallization from toluene solution often yields a mixture of **3·Tol** and guest-free crystals. In the case of the *o*-xylene solution, only small amounts of **3·Xyl** was obtained as a minor product, although a crystal structure of the guest-free crystal was not revealed due to crystal size and mosaicity (Figure S3 in the Supporting Information). On the other hand, crystallization of **3** from chlorobenzene and dichlorobenzene solutions uniquely yielded **3·ClBen** and **3·Cl<sub>2</sub>Ben**. These results indicate that chloro-substituted benzene derivatives are preferably included in the channels because of attractive dispersion forces between the chlorine atoms of the guest and the sp<sup>2</sup>-carbon atoms of the host (Cl- $\pi$  interactions),<sup>[18]</sup> in addition to CH- $\pi$  interactions.<sup>[19]</sup> Figure 3 shows

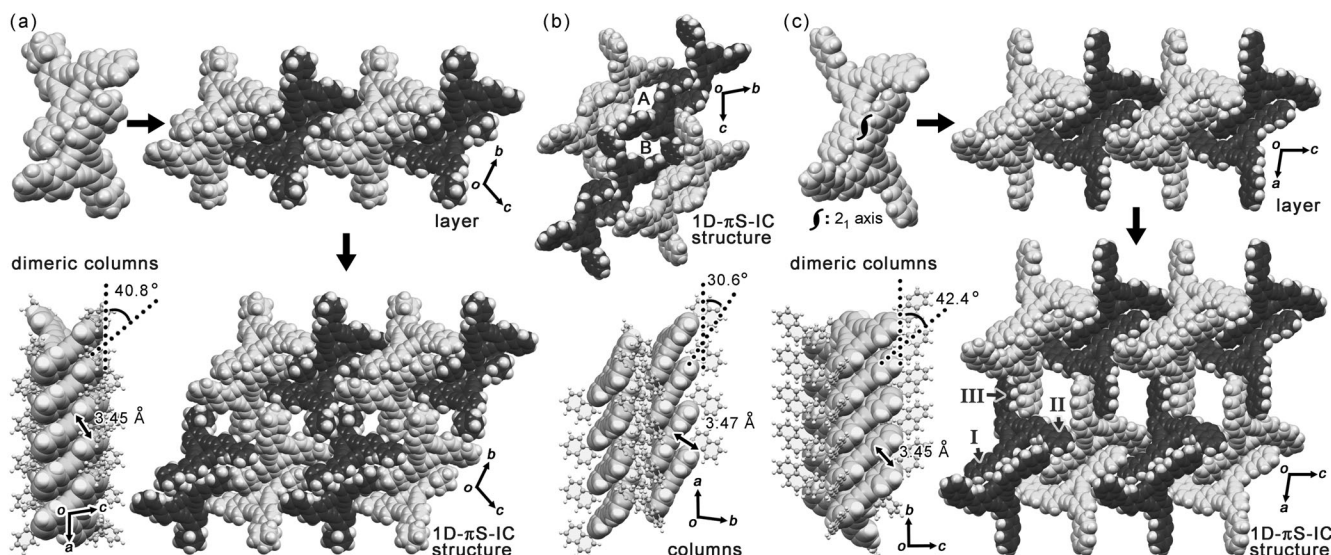


Figure 2. Porous frameworks in the crystals of a) **1·CHCl<sub>3</sub>**, b) **2·Tol**, and c) **3·Tol**. In the case of DBAs **1** (a) and **3** (c), the crystal structures can be interpreted with the use of the hierarchical scenario described in Figure 1. The guest molecules, that is, chloroform for (a), toluene for (b) and (c) in the channels are omitted for clarity. Carbon atoms of DBAs are colored in gray or dark gray for clarity. Two phenyl groups of DBA **1** in (a) are disordered. Geometrical parameters, an angle between a mean plane of the DBA ring and the columnar axis and a distance between mean planes of the stacked DBA rings are shown on the figures of the structures.

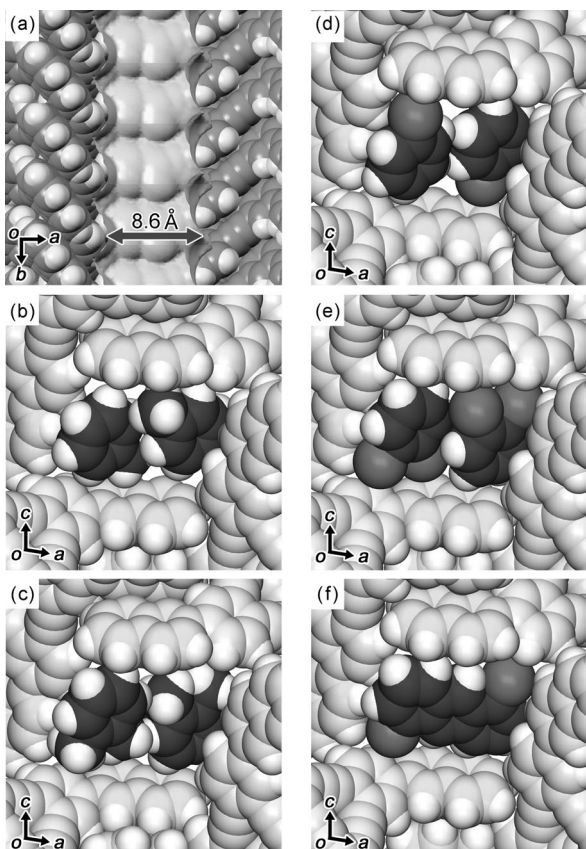


Figure 3. Inclusion-channels-accommodated, aromatic, guest molecules. a) 1D channel in the **2·Tol** crystal visualized by using a probe radius of 1.0 Å. Packing diagrams are focused into the guest molecules: b) **3·Tol**, c) **3·Xyl**, d) **3·ClBen**, e) **3·Cl<sub>2</sub>Ben**, and f) **3·Cl<sub>2</sub>Ant**. Carbon and chlorine atoms of the guests are in black and dark gray, respectively.

the inclusion channels of **3·Tol**, **3·Xyl**, **2·ClBen**, **2·Cl<sub>2</sub>Ben**, and **3·Cl<sub>2</sub>Ant**. The channels have a smooth surface without a narrow bottle neck (the shortest width estimated by a 1.0 Å radius probe is ca. 8.6 Å). Two walls of the rhombic channels are composed of the naphthalene plane, which is convenient to hold aromatic guest molecules through edge-to-face interactions. In the crystals of **3·Tol** and **3·Xyl**, toluene and *o*-xylene molecules interact perpendicularly with the naphthalene walls through CH–π interactions; the dihedral angles are 89.5 and 85.5°, respectively. In the crystals of **3·ClBen** and **3·Cl<sub>2</sub>Ben**, the guest molecules interact perpendicularly with the walls through Cl–π, as well as CH–π, interactions; the dihedral angles are 89.5 and 85.5°, respectively. Because of the effective Cl–π contacts, the latter two inclusion crystals are well stabilized and are obtained exclusively as described above. Furthermore, a larger π system, 1,5-dichloroanthracene, for which the molecular size approximately consists of two coplanarly arranged chlorobenzene molecules, is also accommodated in the channel successfully (the dihedral angle between the naphthalene and anthracene planes is 82.4°).

Interestingly, the crystals that include highly volatile guest molecules, that is, **3·Tol** and **3·ClBen**, spontaneously and gradually release the guests from the channels, even at room temperature. As shown in Figure 4a, freshly prepared crystals of **3·Tol** and **3·ClBen** show gradual weight loss in the thermal gravimetry (TG) curves at 35°C; **3·Tol** and **3·ClBen** lose 92 and 59% of the accommodated guest molecules after 3.5 and 6.5 h, respectively. <sup>1</sup>H NMR spectroscopy also supports guest release: 87 and 67% losses for **3·Tol** and **3·ClBen**, respectively (Figure S5 in the Supporting Information). This behavior is quite a contrast to our previous sys-

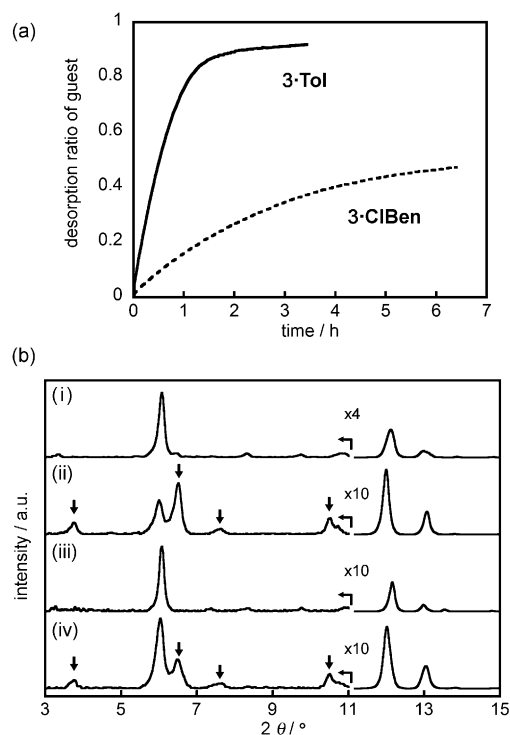


Figure 4. Spontaneous guest desorption of the crystals of **3-Tol** and **3-ClBen** at 35°C accompanied by structural changes. a) Guest desorption curves of **3-Tol** (solid line) and **3-ClBen** (dash line) obtained from TG analysis. b) PXRD patterns of the crystals **3-Tol** (i,ii) and **3-ClBen** (iii,iv) before (i,iii) and after (ii,iv) laying of the crystals at 35°C for 4 and 7 h, respectively.

tems, which have discrete inclusion spaces that accommodates guest molecules (Figure S6 in the Supporting Information).<sup>[8c]</sup> Powder X-ray diffraction ( $\lambda=1.541\text{ \AA}$ , PXRD) patterns of **3-Tol** and **3-ClBen** indicate that guest release provided structural changes as shown in Figure 4b; new peaks appear at 3.7, 6.5, 7.6, and 10.7° upon the guest release. This structural change was also observed for **3-Cl<sub>2</sub>Ben** in addition to **3-Tol** and **3-ClBen** when the crystals were heated (Figure S7 in the Supporting Information). To perform a more precise crystallographic analysis on the structure transformations, PXRD-pattern changes of **3-Tol** were monitored by using synchrotron X-ray diffraction ( $\lambda=1.300\text{ \AA}$ ) under heating conditions. As shown in Figure 5, the peak at 2.84° that corresponds to the (100) plane disappeared, whereas unambiguous peaks at 3.20, 6.40, 6.47, and 8.85° appeared. These spectral changes coincide with those in Figure 4b. The resulting pattern indicates that the *a* and *b* axes shrunk by 2.87 and 0.13 Å, respectively, whereas the *c* axis was elongated by 0.42 Å, and the  $\beta$  angle widened by 1.02°, although the crystalline lattice remains in space group  $P2_1/c$ , as shown in Table S2 in the Supporting Information. Unfortunately, an exact crystal structure with satisfying quality was not achieved by the Rietveld analysis. However, by considering the cell volume and molecular size of **3**, the space to accommodate a guest molecule was collapsed. Upon re-

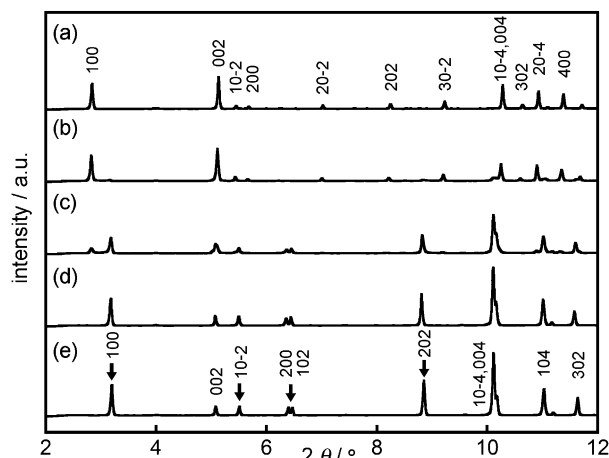


Figure 5. PXRD pattern changes of **3-Tol** upon heating: a) before heating (30°C), at b) 70, c) 90, and d) 110°C, and e) after the sample had been cooled down to 30°C again.

lease of the guest molecules, a fluorescence spectrum of the **3-Tol** crystal is slightly redshifted (Figure S9 in the Supporting Information). This indicates changes of the overlap between the DBA planes.

In summary, we successfully prepared crystals that have both 1D,  $\pi$ -stacked, columnar superstructure and 1D, continuous, inclusion channel accommodating aromatic molecules. Such structures were achieved by symmetry-decreasing crystallization of discotic molecules with  $C_3$  symmetry, namely, DBA derivatives with naphthyl arms. The sterically hindered, rigid naphthalene group yields void spaces surrounded by walls that contain  $\pi$  planes. The guest molecules, toluene and *o*-xylene, are accommodated through CH– $\pi$  contacts in the channels. Furthermore, in the cases of chlorobenzene, *o*-dichlorobenzene, and 1,5-dichloroanthracene, Cl– $\pi$  contacts stabilize guest accommodation. Based on this result, halogen-substituted aromatic compounds with n-type nature might be accommodated in the channels to construct the crystal with the pathways for both electron and hole. We also revealed that inclusion crystals with volatile guest molecules experience spontaneous guest desorption under ambient conditions; this results in shrinkage of the cell. This structural change induced a slight redshift of the fluorescence spectrum.

The present study opens the door for a new category of 1D assemblies of discotic  $\pi$  molecules. A dynamic structural change upon desorption and absorption of guest molecules and guest-dependent physical properties, such as hole mobility, are now investigated in our laboratory.

## Acknowledgements

This work was supported by a Grant-in-Aid for Scientific Research (A 21245035), for Scientific Research on Innovative Areas (22108517), for Challenging Exploratory Research (22651042) by MEXT(Japan). We are

grateful to Dr. K. Miura, Dr. S. Baba, Dr. N. Mizuno, and Dr. K. Osaka for crystallographic data collection at the BL38B1 (proposal No. 2009B1969 and 2010 A1427) and PXRD measurements at BL19B2 (proposal No. 2010B1861 and 2010B1929) in the SPring-8, JASRI. I.H. thanks FRC, Osaka University for funding. N.T. thanks JSPS for a Research Fellowship for Young Scientists.

**Keywords:** aggregation • crystal engineering • dehydrobenzoannulene • inclusion compounds • pi interactions

- [1] Recent reviews, see; a) F. J. M. Hoeben, P. Jonkheijm, E. W. Meijer, A. P. H. J. Schenning, *Chem. Rev.* **2005**, *105*, 1491–1546; b) J. E. Anthony, *Chem. Rev.* **2006**, *106*, 5028–5048; c) T. Kato, N. Mizoshita, K. Kishimoto, *Angew. Chem.* **2006**, *118*, 44–74; *Angew. Chem. Int. Ed.* **2006**, *45*, 38–68; d) J. Wu, W. Pisula, K. Müllen, *Chem. Rev.* **2007**, *107*, 718–747; e) S. Laschat, A. Baro, N. Steinke, F. Giessmann, *Angew. Chem.* **2007**, *119*, 4916–4973; *Angew. Chem. Int. Ed.* **2007**, *46*, 4832–4887; f) L. Zang, Y. Che, J. S. Moore, *Acc. Chem. Res.* **2008**, *41*, 1596–1608; g) F. Würthner, T. E. Kaiser, C. R. Saha-Möller, *Angew. Chem.* **2011**, *123*, 3436–3473; *Angew. Chem. Int. Ed.* **2011**, *50*, 3376–3410.
- [2] a) A. P. Côté, A. I. Benin, N. W. Ockwig, M. O’Keeffe, A. J. Matzger, O. M. Yaghi, *Science* **2005**, *310*, 1166–1170; b) A. P. Côté, H. M. El-Kaderi, H. Furukawa, J. R. Hunt, O. M. Yaghi, *J. Am. Chem. Soc.* **2007**, *129*, 12914–12915; c) S. Wan, J. Guo, J. Kim, H. Ihee, D. Jiang, *Angew. Chem.* **2008**, *120*, 8958–8962; *Angew. Chem. Int. Ed.* **2008**, *47*, 8826–8830; d) S. Wan, J. Guo, J. Kim, H. Ihee, D. Jiang, *Angew. Chem.* **2009**, *121*, 5547–5550; *Angew. Chem. Int. Ed.* **2009**, *48*, 5439–5442; e) S. Patwardhan, A. A. Kocherzhenko, F. C. Grozema, L. D. A. Siebbeles, *J. Phys. Chem. C* **2011**, *115*, 11768–11772.
- [3] a) X. Ding, J. Guo, X. Feng, Y. Honsho, J. Guo, S. Seki, P. Maitarad, A. Saeki, S. Nagase, D. Jiang, *Angew. Chem.* **2011**, *123*, 1325–1329; *Angew. Chem. Int. Ed.* **2011**, *50*, 1289–1293; b) X. Feng, L. Chen, Y. Dong, D. Jiang, *Chem. Commun.* **2011**, *47*, 1979–1981.
- [4] J. W. Colson, A. R. Woll, A. Mukherjee, M. P. Levendorf, E. L. Spitzer, V. B. Shields, M. G. Spencer, J. Park, W. R. Dichtel, *Science* **2011**, *332*, 228–231.
- [5] T. Murata, S. Maki, M. Ohmoto, E. Miyazaki, Y. Umemoto, K. Nakasui, Y. Morita, *CrystEngComm* **2011**, *13*, 6880–6884.
- [6] a) J. L. Atwood, J. E. D. Davies, D. D. MacNichol, *Inclusion Compounds*, Vol. 1–3, Academic Press, London, **1984**; b) F. H. Herbststein, *Crystalline Molecular Complexes and Compounds*, Vol. 1–2, Oxford University Press, Oxford, **2005**.
- [7] a) H. Allcock, *Acc. Chem. Res.* **1978**, *11*, 81–87; b) V. S. S. Kumar, F. C. Pigge, N. P. Rath, *CrystEngComm* **2004**, *6*, 531–534; c) J. A. Riddle, J. C. Bollinger, D. Lee, *Angew. Chem.* **2005**, *117*, 6847–6851; *Angew. Chem. Int. Ed.* **2005**, *44*, 6689–6693; d) C.-K. Lam, F. Xue, J.-P. Zhang, X.-M. Chen, T. C. W. Mak, *J. Am. Chem. Soc.* **2005**, *127*, 11536–11537; e) E. M. García-Frutos, B. Gómez-Lor, Á. Monge, E. Gutiérrez-Puebla, I. Alkorta, J. Elguero, *Chem. Eur. J.* **2008**, *14*, 8555–8561.
- [8] a) A. J. Matzger, M. Shim, K. P. C. Vollhardt, *Chem. Commun.* **1999**, 1871–1872; b) K. Tahara, T. Fujita, M. Sonoda, M. Shiro, Y. Tobe, *J. Am. Chem. Soc.* **2008**, *130*, 14339–14345; c) I. Hisaki, H. Senga, Y. Sakamoto, S. Tuzuki, N. Tohnai, M. Miyata, *Chem. Eur. J.* **2009**, *15*, 13336–13340.
- [9] T. Tozawa, J. T. A. Jones, S. I. Swamy, S. Jiang, D. J. Adams, S. Shakespeare, R. Clowes, D. Bradshaw, T. Hasell, S. Y. Chong, C. Tang, S. Thompson, J. Parker, A. Trewin, J. Bacsa, A. M. Z. Slawin, A. Steiner, A. I. Cooper, *Nat. Mater.* **2009**, *8*, 973–978.
- [10] a) A. Anthony, G. R. Desiraju, R. K. R. Jetti, S. S. Kuduva, N. N. L. Madhavi, A. Nangia, R. Thaimattam, V. R. Thallad, *Cryst. Eng.* **1998**, *1*, 1–18; b) P. K. Thallapally, K. Chakraborty, A. K. Katz, H. L. Carrell, S. Kotha, G. R. Desiraju, *CrystEngComm* **2001**, *3*, 134–136.
- [11] A. I. Kitagorodskii, *Molecular crystals and molecules*, Academic Press, London, **1973**.
- [12] For recent reviews of dehydrobenzoannulene, see: a) U. H. F. Bunz, Y. Rubin, Y. Tobe, *Chem. Soc. Rev.* **1999**, *28*, 107–119; b) C. S. Jones, M. J. O’Connor, M. M. Haley in *Acetylene Chemistry* (Eds.: F. Diederich, P. J. Stang, R. R. Tykwinski), Wiley-VCH, Weinheim, **2005**, pp. 303–385; c) E. L. Spitler, C. A. Johnson II, M. M. Haley, *Chem. Rev.* **2006**, *106*, 5344–5386.
- [13] I. Hisaki, Y. Sakamoto, H. Shigemitsu, N. Tohnai, M. Miyata, S. Seki, A. Saeki, S. Tagawa, *Chem. Eur. J.* **2008**, *14*, 4178–4187.
- [14] S. H. Seo, J. Y. Chang, G. N. Tew, *Angew. Chem.* **2006**, *118*, 7688–7692; *Angew. Chem. Int. Ed.* **2006**, *45*, 7526–7530.
- [15] S. H. Seo, T. V. Jones, H. Seyler, J. O. Peters, T. H. Kim, J. Y. Chang, G. N. Tew, *J. Am. Chem. Soc.* **2006**, *128*, 9264–9265.
- [16] a) K. Tahara, S. Furukawa, H. Uji-i, T. Uchino, T. Ichikawa, J. Zhang, W. Mamduoh, M. Sonoda, F. C. De Schryver, S. De Feyter, Y. Tobe, *J. Am. Chem. Soc.* **2006**, *128*, 16613–16625; b) K. Tahara, H. Yamaga, E. Ghijssens, K. Inukai, J. Adisojoso, M. O. Blunt, S. De Feyter, Y. Tobe, *Nat. Chem.* **2011**, *3*, 714–719.
- [17] Crystal data of **1·CHCl<sub>3</sub>**:  $2(C_{42}H_{24}) \cdot (CHCl_3)$ ,  $M_w = 1176.68$ ,  $a = 5.28110(10)$ ,  $b = 23.0036(2)$ ,  $c = 26.4888(3)$  Å,  $\alpha = 112.7480(4)^\circ$ ,  $\beta = 95.7280(4)^\circ$ ,  $\gamma = 96.5920(6)^\circ$ ,  $V = 2911.29(7)$  Å<sup>3</sup>,  $T = 100$  K, triclinic, space group *P-1* (No. 2),  $Z = 2$ ,  $d_{\text{calcd}} = 1.342$  g cm<sup>-3</sup>, 54105 collected, 14266 unique ( $R_{\text{int}} = 0.062$ ) reflections, the final *R*1 and *wR*2 values 0.092 ( $I > 2.0\sigma(I)$ ) and 0.271 (all data), respectively. Crystal data for **2·Tol**:  $(C_{54}H_{30})_2(C_7H_8)_{0.5}$ ,  $M_w = 770.97$ ,  $a = 6.8192(2)$ ,  $b = 15.9473(6)$ ,  $c = 19.8688(9)$  Å,  $\alpha = 100.0360(17)^\circ$ ,  $\beta = 99.4874(18)^\circ$ ,  $\gamma = 95.561(3)^\circ$ ,  $V = 2080.89(14)$  Å<sup>3</sup>,  $T = 100$  K, triclinic, space group *P-1* (No. 2),  $Z = 2$ ,  $d_{\text{calcd}} = 1.232$  g cm<sup>-3</sup>, 34385 collected, 7990 unique ( $R_{\text{int}} = 0.056$ ) reflections, the final *R*1 and *wR*2 values 0.092 ( $I > 2.0\sigma(I)$ ) and 0.268 (all data), respectively. Crystal data for **3·Tol**:  $(C_{54}H_{30}) \cdot (C_7H_8)_3$ ,  $M_w = 770.97$ ,  $a = 26.3124(4)$ ,  $b = 5.24830(10)$ ,  $c = 29.1901(5)$  Å,  $\alpha = 90^\circ$ ,  $\beta = 99.2125(6)^\circ$ ,  $\gamma = 90^\circ$ ,  $V = 3979.02(12)$  Å<sup>3</sup>,  $T = 100$  K, monoclinic, space group *P2<sub>1</sub>/c* (No. 14),  $Z = 4$ ,  $d_{\text{calcd}} = 1.287$  g cm<sup>-3</sup>, 36354 collected, 10536 unique ( $R_{\text{int}} = 0.080$ ) reflections, the final *R*1 and *wR*2 values 0.092 ( $I > 2.0\sigma(I)$ ) and 0.219 (all data), respectively. Crystal data for **3·Xyl**:  $(C_{54}H_{30}) \cdot (C_8H_{10})$ ,  $M_w = 785.00$ ,  $a = 26.4700(4)$ ,  $b = 5.28000(10)$ ,  $c = 29.1935(5)$  Å,  $\alpha = 90^\circ$ ,  $\beta = 98.4027(6)^\circ$ ,  $\gamma = 90^\circ$ ,  $V = 4036.33(12)$  Å<sup>3</sup>,  $T = 100$  K, monoclinic, space group *P2<sub>1</sub>/c* (No. 14),  $Z = 4$ ,  $d_{\text{calcd}} = 1.292$  g cm<sup>-3</sup>, 28566 collected, 8433 unique ( $R_{\text{int}} = 0.055$ ) reflections, the final *R*1 and *wR*2 values 0.065 ( $I > 2.0\sigma(I)$ ) and 0.194 (all data), respectively. Crystal data for **3·ClBen**:  $(C_{54}H_{30}) \cdot (C_6H_5Cl)$ ,  $M_w = 791.39$ ,  $a = 26.1957(2)$ ,  $b = 5.2068(1)$ ,  $c = 29.2486(3)$  Å,  $\alpha = 90^\circ$ ,  $\beta = 99.0907(3)^\circ$ ,  $\gamma = 90^\circ$ ,  $V = 3939.28(5)$  Å<sup>3</sup>,  $T = 100$  K, monoclinic, space group *P2<sub>1</sub>/c* (No. 14),  $Z = 4$ ,  $d_{\text{calcd}} = 1.334$  g cm<sup>-3</sup>, 32531 collected, 8788 unique ( $R_{\text{int}} = 0.038$ ) reflections, the final *R*1 and *wR*2 values 0.041 ( $I > 2.0\sigma(I)$ ) and 0.111 (all data), respectively. Crystal data for **3·Cl<sub>2</sub>Ben**:  $(C_{54}H_{30}) \cdot (C_6H_4Cl_2)$ ,  $M_w = 825.83$ ,  $a = 26.5396(2)$ ,  $b = 5.1592(1)$ ,  $c = 29.5302(3)$  Å,  $\alpha = 90^\circ$ ,  $\beta = 98.8797(3)^\circ$ ,  $\gamma = 90^\circ$ ,  $V = 3994.91(10)$  Å<sup>3</sup>,  $T = 100$  K, monoclinic, space group *P2<sub>1</sub>/c* (No. 14),  $Z = 4$ ,  $d_{\text{calcd}} = 1.373$  g cm<sup>-3</sup>, 33252 collected, 9276 unique ( $R_{\text{int}} = 0.043$ ) reflections, the final *R*1 and *wR*2 values 0.064 ( $I > 2.0\sigma(I)$ ) and 0.191 (all data), respectively. Crystal data for **3·Cl<sub>2</sub>Ant**:  $(C_{54}H_{30}) \cdot (C_{14}H_8Cl_2)_{0.5}$ ,  $M_w = 802.39$ ,  $a = 26.4636(3)$ ,  $b = 5.12230(10)$ ,  $c = 29.4798(4)$  Å,  $\alpha = 90^\circ$ ,  $\beta = 99.2825(5)^\circ$ ,  $\gamma = 90^\circ$ ,  $V = 3943.79(11)$  Å<sup>3</sup>,  $T = 100$  K, monoclinic, space group *P2<sub>1</sub>/c* (No. 14),  $Z = 4$ ,  $d_{\text{calcd}} = 1.351$  g cm<sup>-3</sup>, 21301 collected, 8255 unique ( $R_{\text{int}} = 0.095$ ) reflections, the final *R*1 and *wR*2 values 0.086 ( $I > 2.0\sigma(I)$ ) and 0.249 (all data), respectively. CCDC-846846 (**1·CHCl<sub>3</sub>**), CCDC-846847 (**2·Tol**), CCDC-846848 (**3·Tol**), CCDC-846849 (**3·Xyl**), CCDC-846850 (**3·ClBen**), CCDC-846851 (**3·Cl<sub>2</sub>Ben**), and CCDC-846852 (**3·Cl<sub>2</sub>Ant**) contain the supplementary crystallographic data for this paper. These data can be obtained free of charge from The Cambridge Crystallographic Data Centre via [www.ccdc.cam.ac.uk/data\\_request/cif](http://www.ccdc.cam.ac.uk/data_request/cif).
- [18] For reviews, see: a) G. R. Desiraju, T. Steiner, *The Weak Hydrogen Bond in Structural Chemistry and Biology*, Oxford University Press, Oxford, **1999**; b) M. Nishio, *CrystEngComm* **2004**, *6*, 130–158; c) S. Tsuzuki, A. Fujii, *Phys. Chem. Chem. Phys.* **2008**, *10*, 2584–2594.

- [19] a) S. Tsuzuki, K. Honda, T. Uchimaru, M. Mikami, K. Tanabe, *J. Phys. Chem. A* **1999**, *103*, 8265–8271; b) S. Tsuzuki, K. Honda, T. Uchimaru, M. Mikami, K. Tanabe, *J. Am. Chem. Soc.* **2000**, *122*, 3746–3753; c) K. Shibasaki, A. Fujii, M. Mikami, S. Tsuzuki, *J. Phys. Chem. A* **2007**, *111*, 753–758.

Received: October 5, 2011

Published online: November 23, 2011